Available online at www.sciencedirect.com
ScienceDirect
Progress in Natural Science 18 (2008) 661–664
Progress in Natural Science
www.elsevier.com/locate/pnsc

Effect of Tm–Er concentration ratio on the photoluminescence of Er–Tm:Al_2O_3 thin films fabricated by pulsed laser deposition

Bo Zhou [a], Zhisong Xiao [a,*], Anping Huang [a], Lu Yan [a], Fang Zhu [a], Jinliang Wang [a], Penggang Yin [b], Hao Wang [c]

[a] *Department of Physics, School of Science, Beihang University, Beijing 100083, China*
[b] *School of Materials Science and Engineering, Beihang University, Beijing 100083, China*
[c] *Faculty of Physics and Electronics, Hubei University, Wuhan 430062, China*

Received 10 September 2007; received in revised form 4 January 2008; accepted 9 January 2008

Abstract

Er–Tm codoped amorphous aluminum oxide (a-Al_2O_3) thin films have been prepared by an alternative pulsed laser deposition. The phase structure and the surface of the deposited thin films were characterized by the X-ray diffraction (XRD) and scanning electron microscopy (SEM), respectively. Effective photoluminescence (PL) in the region of 350–900 nm was observed when pumped at 325 nm, and the PL performance has been improved by modifying the Tm^{3+} concentration. With the increasing of [Tm]/[Er] concentration ratio, the intensity of emission of 382 nm and 500 nm bands was improved effectively while that of 765 nm band increased smoothly. Our results suggest that the resonant energy transfer and cross relaxation between Tm^{3+} and Er^{3+} play an important role in the evolution of the luminescent response.

Keywords: Tm; Er; Concentration; Photoluminescence; Energy transfer

1. Introduction

Rare earth (RE) ions such as erbium (Er^{3+}) and thulium (Tm^{3+}) have attracted much attention in both visible and infrared regions for their unique energy levels [1–4]. The transition of Er^{3+} $^4I_{13/2} \rightarrow {}^4I_{15/2}$ has been successfully applied in the amplification of Er-doped fiber amplifiers (EDFAs) and Er-doped waveguide amplifiers (EDWAs) in optical communication systems corresponding to 1.54 μm photon, which is located in the low loss "window" of silica-based optical fibers [2–4]. On the other hand, upconversion of infrared light to visible light by rare earth ions doped materials have also been investigated extensively due to the potential applications in display materials and devices, on which good multicolor has been achieved in Er/Tm/Yb-doped tellurite glasses [5] and oxyfluoride glass ceramics [6]. The content of rare earth ions plays an important role in the upconversion of infrared light to visible light. The aim of this study is to investigate the effect of Tm–Er concentration ratio on the photoluminescence of Er–Tm codoped thin films in the wavelength range of 350–900 nm.

Pulsed laser deposition (PLD) has been proved to be excellent for the preparation of complex oxides, which are the basic materials used for the preparation of waveguide structure [7,8]. PLD involves high kinetic energy species, which enable the production of high density films with good adhesion [9]. These unique features make PLD very attractive for the deposition of optical thin films, especially for the nanostructured thin films [10]. The a-Al_2O_3 is a promising material for the thin film applications due to

* Corresponding author. Tel./fax: +86 10 82317935.
E-mail address: zsxiao@buaa.edu.cn (Z. Xiao).

1002-0071/$ - see front matter © 2008 National Natural Science Foundation of China and Chinese Academy of Sciences. Published by Elsevier Limited and Science in China Press. All rights reserved.
doi:10.1016/j.pnsc.2008.01.009

its high thermal conductivity, excellent mechanical properties and a wide range of transparency [11]. Flat and wide infrared emissions have been achieved in Er–Tm codoped Al_2O_3 thin films prepared by PLD [12,13], where the RE ions are dispersed separately on nanoscale in depth in a-Al_2O_3.

In this study, Er and Tm codoped Al_2O_3 thin films were prepared by PLD in which the distributions of Er and Tm ions were nanostructured, and the effect of Tm–Er concentration ratio on the luminescence was investigated.

2. Experiment

The Er–Tm codoped Al_2O_3 thin films have been prepared on Si(100) substrate at room temperature by PLD. An KrF excimer laser ($\lambda = 248$ nm, $\tau = 15$ ns full width at half maximum) was used to alternatively ablate the ceramic targets of Er:Al_2O_3 (0.80 mol%) and Tm:Al_2O_3 (2.40 mol%). The thin films of multi-layer structure [14] were deposited with total film thickness of about 100 nm. Fig. 1 schematically shows the nanostructure of the thin films. The thickness of Er-doped layer was designated to be constant and equal to 1.2 nm in every unit, and the Tm-doped layer was changed from 0.4, 0.8, 1.6 to 2 nm to adjust the Tm–Er concentration ratio (corresponding to [Tm]/[Er] of 1, 2, 4 and 5, respectively). The total film thickness was kept constant to compare the PL properties of the thin films.

The concentrations of Er^{3+} and Tm^{3+} were fixed at 7.2×10^{19} cm^{-3} and 2.2×10^{20} cm^{-3} based on the dopants concentration in RE-doped targets, which is consistent with the results measured by Rutherford backscattering spectrometry (RBS). All the deposited films were rapidly annealed in air at 800 °C for 50 s. PL measurements were performed at room temperature using a single grating monochromator, a microscopic confocal Raman spectrometer and the standard lock-in techniques, and pumped at the wavelength of 325 nm from a He–Cd laser. The scanning region is from 350 to 900 nm.

The phase structure of Al_2O_3 in the deposited film was investigated by X-ray diffraction (XRD) and the surface of the thin film was determined by scanning electron microscopy (SEM).

3. Results and discussion

Fig. 2 shows the XRD pattern of the Er–Tm codoped Al_2O_3 thin films. There is only one diffractive peak coming from Si(200), and no peak corresponding to α- or γ- or θ-Al_2O_3 phase has been observed. This means that the as-deposited films are amorphous, which could induce to a relative broadband PL of Er^{3+} and Tm^{3+} ions in Al_2O_3 host. This is consistent with the result in Ref. [13]. Fig. 3 shows the SEM image of Er–Tm codoped Al_2O_3 thin films rapidly annealed for 50 s in air at 800 °C. The flat surface morphology was observed as shown in Fig. 3, which is the same as the result obtained by Song et al. [15].

Fig. 4 shows the PL spectra of Er–Tm codoped Al_2O_3 thin films with [Tm]/[Er] concentration ratios (R) of 1, 2, 4 and 5, respectively. Three distinct emissions in the PL spectra located at 382 nm, 491–512 nm and 761–765 nm (denoted by A, B and C band, respectively) were observed as shown in Fig. 3. The emission band B is composed of several emission peaks located in the band 491–512 nm with full width at half maximum (FWHM) of ~90 nm. There are two weak emissions peaked at 410 and 435 nm between A and B bands, and a 562 nm shoulder peak beside the right of B emission band can be observed (Fig. 4).

The PL intensities of emissions A and B increased with the increasing of [Tm]/[Er] concentration ratio, and intensities of B increased in a steeper rate compared to that of peak A when [Tm]/[Er] increased from 4 to 5, while that of peak C increased smoothly all the time (Fig. 5). These results mean that the high [Tm]/[Er] ratio can only improve the PL performance of emissions A and B, and exerts little effect on that of C. Among these three emission bands, peak A is the sharpest and B exhibits a wide band with the increasing of [Tm]/[Er], which means that the local environment of the RE ions-occupied Al_2O_3 matrix is different [16,17]. Details about the three emissions related to the corresponding transitions will be discussed in what follows.

Er^{3+} and Tm^{3+} were excited to the corresponding states when pumped at a wavelength of 325 nm, and emitted pho-

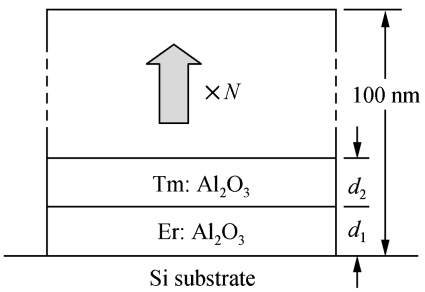

Fig. 1. Schematic structure of the Er–Tm codoped Al_2O_3 thin films with different [Tm]/[Er] concentration ratios of 1, 2, 4 and 5, respectively.

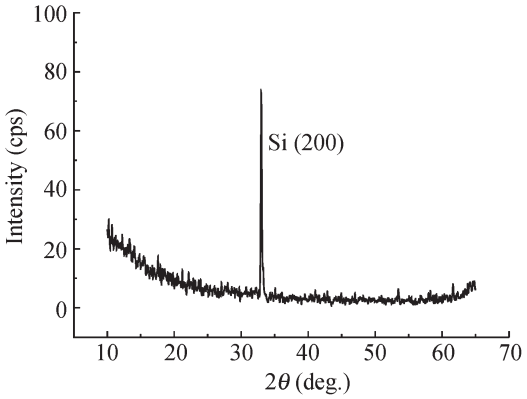

Fig. 2. The XRD pattern of the Er–Tm codoped Al_2O_3 thin films with [Tm]/[Er] concentration ratio of 2.

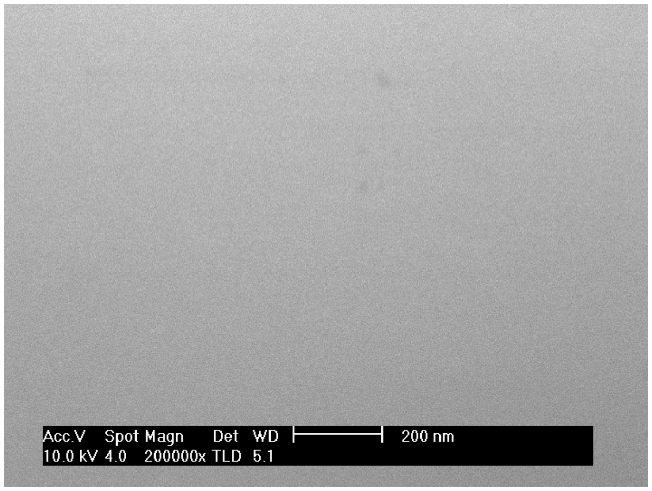

Fig. 3. The surface image of Er–Tm codoped Al_2O_3 thin films rapidly annealed for 50 s in air at 800 °C.

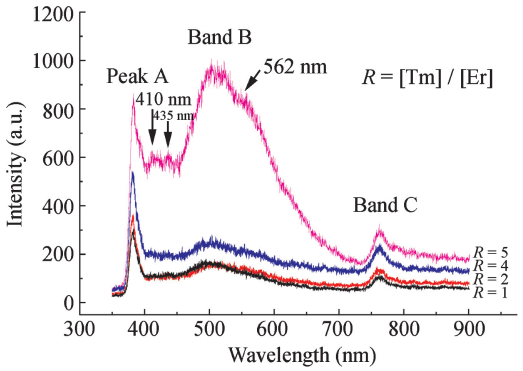

Fig. 4. PL spectra of Er–Tm codoped Al_2O_3 thin films with [Tm]/[Er] concentration ratios of 1, 2, 4 and 5, respectively.

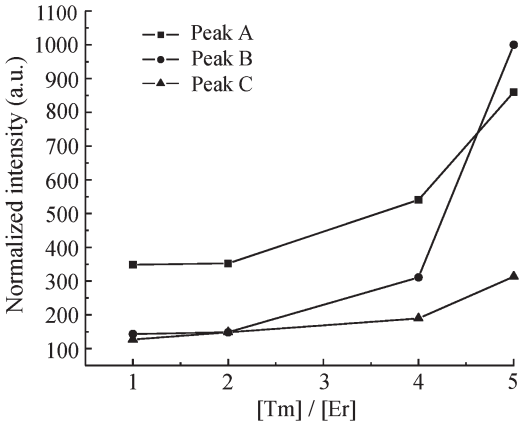

Fig. 5. PL intensity of Er–Tm codoped Al_2O_3 thin films with [Tm]/[Er] concentration ratios of 1, 2, 4 and 5, respectively.

tons when they radiatively decayed to lower states or ground state. For Er^{3+}, after absorbing the pumping energy they were pumped up to the $^4F_{3/2}$ state, and then rapidly relaxed to the $^4G_{11/2}$ state, which radiatively decayed to the first excited state $^4I_{13/2}$ or ground state $^4I_{15/2}$ with the emission peaks corresponding to 505 nm or 382 nm photons. As well, some ions may be nonradiatively relaxed to state $^4F_{7/2}$ in a phonon-assisted way (the phonon energy of Al_2O_3 is about 870 cm^{-1}), and then transited to state $^4I_{13/2}$ or $^4I_{15/2}$, emitting 765 nm or 512 nm photons. For Tm^{3+}, after the absorption of the pumping photons, they rapidly relaxed to the $^1D_2$ state, and then transited to the $^3H_5$ or $^3F_3$ state, emitting 509 nm and 765 nm photons, and the transition $^1G_4 \rightarrow {}^3H_5$ can also emit the 765 nm photons. All the possible transitions in both Er^{3+} and Tm^{3+} are illustrated in Fig. 6.

Only the transition $^4G_{11/2} \rightarrow {}^4I_{15/2}$ of Er^{3+} corresponding to 382 nm photon is found in Fig. 6 and there is no corresponding transition in Tm^{3+}. The PL intensity of 382 nm increased with the increasing [Tm]/[Er], while the Er content decreased. To understand the observed results, it is necessary to assume that an energy transfer process takes place between Er^{3+} and Tm^{3+}. The distance of RE ions and the matched energy levels are two important factors improving the probability of energy transfer based on Dexter's calculation [18]. It can be seen from Fig. 6 that the energy levels $^2G_{7/2}$ of Er^{3+} and $^1D_2$ of Tm^{3+} are resonant, the mean distance between RE ions are from 1.5 to 0.9 nm calculated by the fixed RE-doping concentration, assuming that the RE ions are distributed uniformly in every layer. The small neighboring distance and the resonant levels of Tm^{3+} ($^1D_2$) and Er^{3+} ($^2G_{7/2}$) made this energy transfer Tm^{3+} ($^1D_2$) $\rightarrow$ Er^{3+} ($^2G_{7/2}$) (denoted by ET in Fig. 6) easily achievable, and then populated Er^{3+} on state $^4G_{11/2}$, and finally enhanced the PL performance of 382 nm emission by increasing the ratio of [Tm]/[Er] from 1 to 5.

For the B emission band, the transitions of $^4G_{11/2} \rightarrow {}^4I_{13/2}$, $^4F_{7/2} \rightarrow {}^4I_{15/2}$ and $^1D_2 \rightarrow {}^3H_5$, $^1G_4 \rightarrow {}^1D_2$ can emit photons in this wavelength range. The rapid increase of PL intensity with the increasing [Tm]/[Er] indicates that the B emission mainly results from the transition of Tm^{3+}. The fluorescence branch ratio of $^1G_4 \rightarrow {}^3H_5$ is too small to be considered [19], therein the B emission comes from the transition $^1D_2 \rightarrow {}^1G_4$. Fig. 6 shows that the energy difference between $^1D_2$ and $^1G_4$ is large and the

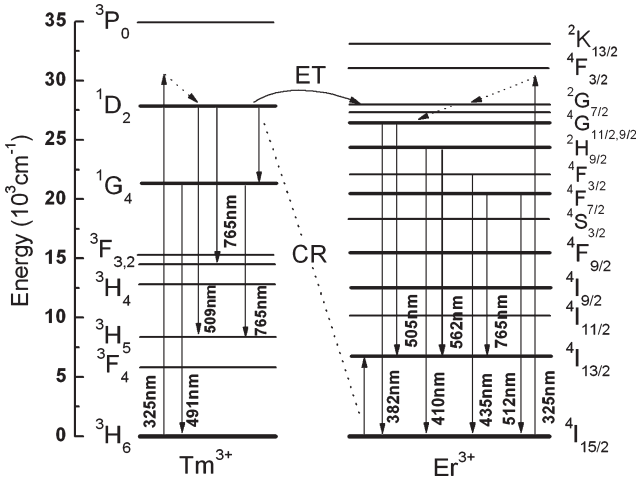

Fig. 6. The energy levels diagram of Er^{3+} and Tm^{3+} ions, and possible transitions between the RE ions.

relaxation of Tm^{3+} from $^1D_2$ to $^1G_4$ can be ignored. Considering that the energy mismatch of $^1D_2 \rightarrow {}^1G_4$ and $^4I_{15/2} \rightarrow {}^4I_{13/2}$ is small, we suggest that more Tm ($^1G_4$) ions are populated by the cross relaxation Tm^{3+} ($^1D_2$), Er^{3+} ($^4I_{15/2}$) → Tm^{3+} ($^1G_4$), Er^{3+} ($^4I_{13/2}$) (denoted by CR in Fig. 6), which increases the number of Tm^{3+} ($^1G_4$), and enhances the B emission.

We can also find that the transitions of Er^{3+} $^4F_{7/2} \rightarrow {}^4I_{13/2}$ and Tm^{3+} $^1D_2 \rightarrow {}^3F_3$, $^1G_4 \rightarrow {}^3H_5$ can emit the 765 nm photons. The PL intensity increases slowly with the [Tm]/[Er], which means that the C emission is not mainly contributed from Tm^{3+}. The branch ratio of $^1D_2 \rightarrow {}^3F_3$ is too little to be considered [19], while that of the transition $^1G_4 \rightarrow {}^3H_5$ varied from 13% to 27% (for $^1G_4 \rightarrow {}^3H_6$ is large than 50%) [19–21] emits the 765 nm photons. The Tm^{3+} in $^1G_4$ state is populated by the cross relaxation mentioned above. For Er^{3+}, the branch ratio of $^4F_{7/2} \rightarrow {}^4I_{13/2}$ is 9–17% [22–24], which can also emit 765 nm photons. Thus, the C emission band comes mainly from both the transitions of Er^{3+} $^4F_{7/2} \rightarrow {}^4I_{13/2}$ and Tm^{3+} $^1G_4 \rightarrow {}^3H_5$.

It should be noted that there are other kinds of interaction among the Er^{3+}, Tm^{3+} and host materials, although we clarify the light-emitting channels of the three emission bands in our samples. Many other measurements are necessary to further investigate the visible luminescence of RE ions in a-Al_2O_3 matrix.

4. Conclusion

Er–Tm codoped amorphous Al_2O_3 thin films have been fabricated by alternatively ablating the ceramic Er:Al_2O_3 and Tm:Al_2O_3 targets, and the PL performance of Er and Tm ions has been improved by adjusting the concentrations of RE dopants. The energy transfer processes between Er^{3+} and Tm^{3+} have been proposed to interpret the enhancement of the visible emission peaks by increasing the [Tm]/[Er] concentration ratio from 1 to 5 under 325 nm pumping. The results evidence the energy transfer and cross relaxation between Er^{3+} and Tm^{3+}, which could be controlled to tailor the PL response. Further studies are necessary to optimize the concentration and distribution of dopants to adjust the energy exchange interaction between RE ions and to obtain more effective emission.

Acknowledgements

This work was supported by the National Natural Science Foundation of China (Grant Nos. 10604003 and 50772006), the Beijing Nova Project (Grant No. 2006B15) and the Program for New Century Excellent Talents in University (NCET-07-0045).

References

[1] Polman A. Erbium implanted thin film photonic materials. J Appl Phys 1997;82(1):1–39.

[2] Kani J, Hattori K, Jinno M, et al. Trinal-wavelength-band WDM transmission over dispersion-shifted-fiber. Electron Lett 1999;35(4):321–2.

[3] Naftaly M, Shen S, Jha A. Tm^{3+}-doped tellurite glass for a broadband amplifier at 1.47 μm. Appl Opt 2000;39(27):4979–81.

[4] Jeong H, Oha K, Han SR, et al. Characterization of broadband amplified spontaneous emission from an Er^{3+}–Tm^{3+} co-doped silica fiber. Chem Phys Lett 2003;367(3–4):507–11.

[5] Xu SQ, Ma HP, Fang DW, et al. Tm^{3+}/Er^{3+}/Yb^{3+}-codoped oxyhalide tellurite glasses as materials for three-dimensional display. Mater Lett 2005;59:3066–8.

[6] Duan ZC, Zhang JJ, Xiang WD, et al. Multicolor upconversion of Tm^{3+}/Er^{3+}/Yb^{3+} doped oxyflouride glass ceramics. Mater Lett 2007;61(11–12):2200–3.

[7] Smulovich J. Rare-earth-doped devices. In: Proceedings of SPIE, vol. 2996, 1997, p. 143–53.

[8] Grivas C, May-Smith TC, Shepherd DP, et al. Laser operation of a low loss (0.1 dB/cm) Nd:$Gd_3Ga_5O_{12}$ thick (40 micron) planar waveguide grown by pulsed laser deposition. Opt Commun 2004;229(1–6):355–61.

[9] Singh RK, Narayan J. Pulsed laser evaporation technique for deposition of thin films: physics and theoretical model. Phys Rev B 1990;41(13):8843–59.

[10] Seo SY, Shin JH. Controlling Er–Tm interaction in Er and Tm codoped silicon-rich silicon oxide using nanometer-scale spatial separation for efficient, broadband infrared luminescence. Appl Phys Lett 2004;85(18):4151–3.

[11] Lee MB, Lee JH, Frederick BG, et al. Surface structure of ultra-thin Al_2O_3 films on metal substrates. Surf Sci 2000;448(2–3):L207–12.

[12] Xiao ZS, Serna R, Afoson CN, et al. Broadband infrared emission from Er–Tm:Al_2O_3 thin films. Appl Phys Lett 2005;87(11):111103–5.

[13] Xiao ZS, Serna R, Afoson CN. Broadband emission in Er–Tm co-doped Al_2O_3 films: the role of energy transfer from Er to Tm. J Appl Phys 2007;101(3):033112–7.

[14] Serna R, de Castro MJ, Chaos JA, et al. Photoluminescence performance of pulsed laser deposited Al_2O_3 thin films with large erbium concentrations. J Appl Phys 2001;90(10):5120–5.

[15] Song Q, Li CL, Li JY, et al. Photoluminescence properties of Yb:Er co-doped Al_2O_3 thin film fabricated by microwave ECR plasma source enhanced RF magnetron sputtering. Opt Mater 2006;28:1344–9.

[16] Hayashi H, Tanabe S, Hanada T. 1.4 μm band emission properties of Tm^{3+} ions in transparent glass ceramics containing PbF_2 nanocrystals for S-band amplifier. J Appl Phys 2001;89(2):1041–5.

[17] van den Hoven GN, Snoeks E, Polman A, et al. Photoluminescence characterization of Er-implanted Al_2O_3 films. Appl Phys Lett 1993;62(24):3065–7.

[18] Dexter DL. A theory of sensitized luminescence in solids. J Chem Phys 1953;21(5):836–50.

[19] Walsh BM, Barnes NP, Reichle DJ, et al. Optical properties of Tm^{3+} ions in alkali germinate glass. J Non-Cryst Solids 2006;352:5344–52.

[20] Rai VK, de S Menezes L, de Araujo CB. Spectroscopy, energy transfer, and frequency upconversion in Tm^{3+}-doped TeO_2-PbO glass. J Appl Phys 2007;102(4):043505–8.

[21] Giri NK, Singh AK, Rai SB. Judd-Ofelt analysis of Tm and energy transfer studies between Tm and Er codoped in lithium tellurite network. Spectrochim Acta A 2007;68:117–22.

[22] Sardar DK, Dee DM, Nash KL, et al. Absorption intensities and emission cross section of intermanifold transition of Er^{3+}:Y_2O_3 nanocrystals. J Appl Phys 2007;101(11):083105–10.

[23] Sardar DK, Nash KL, Yow RM, et al. Optical characterization and ligand-field splitting of Er^{3+} ($4f^{11}$) energy levels in a fluorine containing tellurite glass. J Appl Phys 2007;102(8):113115–9.

[24] Brito TB, Vermelho MVD, Gouveia EA, et al. Optical characterization of Nd^{3+}- and Er^{3+}-doped lead-indium-phosphate glasses. J Appl Phys 2007;102(4):043113–9.